UPCommons

Portal del coneixement obert de la UPC

http://upcommons.upc.edu/e-prints

Evaluating drape shape in woven fabrics

E.Carrera-Gallissà[a*], X.Capdevila[a], J.Valldeperas[b]

[a]Departamento de Ingeniería Textil y Papelera, Universitat Politècnica de Catalunya, Terrassa (Barcelona), Spain
[b]Instituto de Investigación Textil y Cooperación Industrial de Terrassa, Universitat Politècnica de Catalunya, Terrassa (Barcelona), Spain

*Corresponding autor: Email: carrera @catunesco.upc.edu

Evaluating drape shape in woven fabrics

A search of the scientific literature for the period 1950–2013 retrieved 36 different drape indicators. Despite the large number of indicators currently available, the drape ratio (%DR) continues to be the most widely used, even though it has proved inadequate to explain drape shape. In order to assess their actual performance, the 36 currently existing drape indicators were determined in a total of 37 commercial drapery, woolmaking, shirtmaking and lining woven fabrics spanning a wide range of composition, aerial weight and weave type by using a digital Cusick drape meter. A correlation analysis between indicators, and subsequent suppression of duplicity and collinearity, revealed that seven were mutually correlated. A principal component analysis of the results revealed an underlying structure consisting of three common factors which allowed the indicators to be classified into three different groups according to drape intensity (a), severity (b), and shape symmetry and variability (c). Cluster analysis was additionally used to examine the results in graphical form and exposed three clusters coinciding with the three factors of the underlying structure. A criterion for distinguishing fabrics with an identical drape ratio in terms of drape shape based on sequential application of four of the seven initially selected indicators was developed and experimentally validated.

Key words: *Drape Indicators, drape shape, woven fabrics, factor analysis, cluster analysis.*

Introduction

Like fabric hand, consumers assess fabric drape subjectively (by visual inspection or feeling). Because the sensations consumers can acquire in this way can determine their appreciation of fabrics, the ability to assess fabric drape in an objective manner has considerable industrial, economic and commercial interest. Although drape is determined visually, it is usually assessed subjectively according to social, cultural and historical patterns that change in time (fashion) and space (geographic location).

The first drape meter (Chu, Cummings, & Teixeira,1950), was subsequently improved and eventually adopted for assessing this fabric property by most standardization agencies (Cusick, 1962, 1965, 1968), Figure 1 shows a typical drape meter.
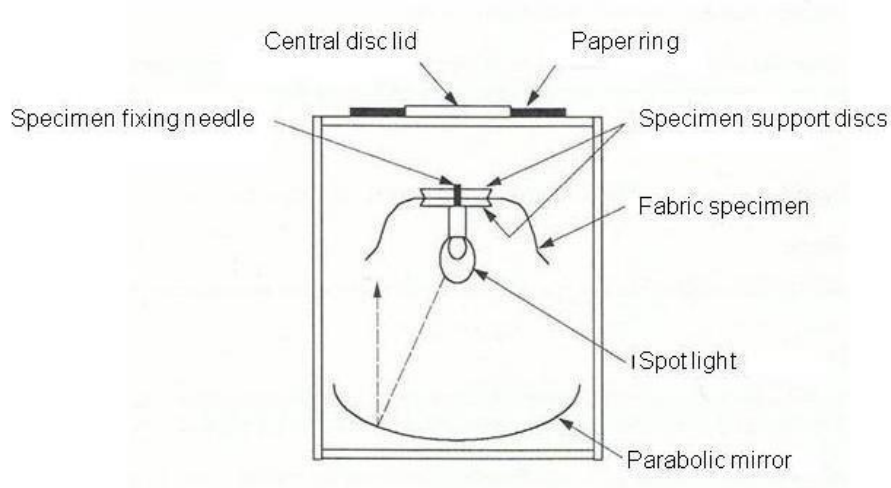
Figure 1. Functioning principle of the Cusick drape meter

Drape meters are used to calculate the drape ratio (*%DR*), which is defined as follows (equation 1):

$$\%DR = \frac{Specimen\ projected\ area - Support\ disc\ area}{Specimen\ area - Support\ disc\ area} \times 100 \qquad (1)$$

Although this indicator provides an accurate measure of drape, it fails to discriminate between drape profiles for fabrics with a very similar *%DR* value.

Existing drape indicators

Ever since the original fabric drape meter was developed in the mid-1950s, textile researchers have proposed a variety of drape indicators that are described below.

a) Fold number, *FN* (Chu, Platt & Hamburguer, 1960). A fold is defined here as the maximum of the projection of the drape profile on a plane. Geometrically, folds are roughly triangles of width *FW* and height FH having a peak (FP) and two adjacent valleys (FV) as vertices (see Figure 2).
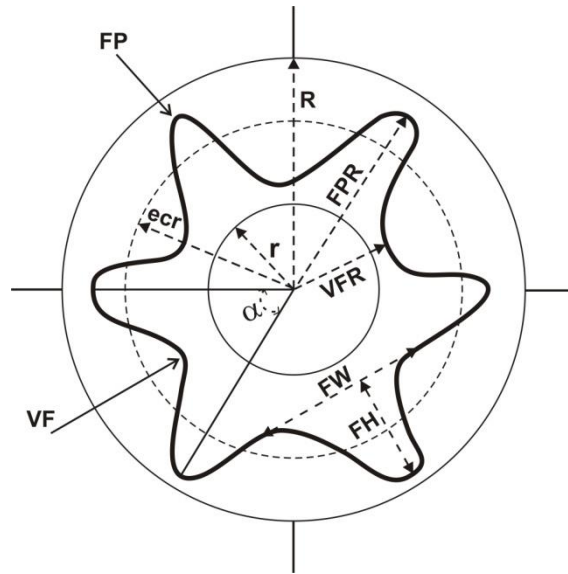
Figure 2. *FP* = fold peak, VF = valley fold, *FPR* = fold peak radius, *VFR* = valley fold radius, *FW* = fold width, *FH* = fold height, *r* = support disc radius, *R* = specimen radius, *ecr* = equivalent circle radius, α = angle between consecutive folds.

b) <u>Shape Factor</u>, *SF* (Chu, Platt & Hamburguer, 1960). The difficulty of calculating fold shape in a simple, reproducible manner led the proponents of this indicator to develop a simplified version assuming all folds in a specimen to be identical and symmetric. *SF* is calculated as the amplitude-to-length ratio of the wave formed by folds on the assumption that all folds are identical. In this work, it was calculated as the ratio of the mean peak length (*FaPR*) to wavelength (*l*) (see Figure 3). *SF*, which is expressed in mm, was computed from the following equation, based on Figure 7 and the cosine theorem:

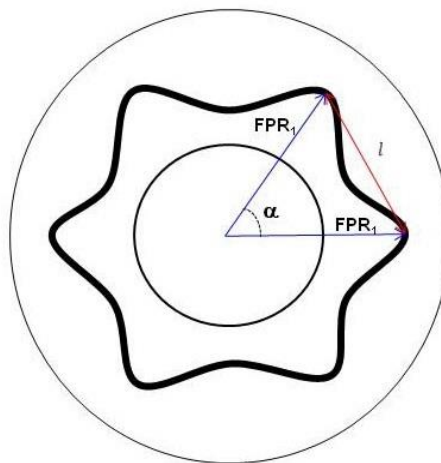$$SF = \frac{FPR1}{\sqrt[2]{2\,FPR1^2(1-\cos a)}} \qquad (2)$$

Figure 3. Trigonometric principle behind the calculation of the shape factor

c) Drape ratio, *%DR* (Cusick, 1968). This is the most widely used indicator even though it fails to discriminate between drape shapes in some cases (Figure 4). Mathematically, the drape ratio is calculated as follows:

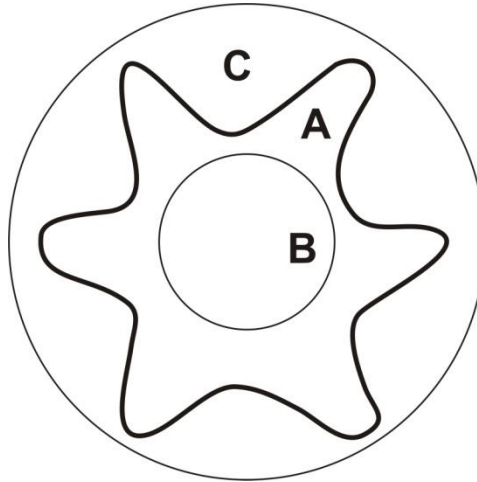$$DR\% = \left(\frac{A-B}{C-B}\right) \cdot 100 \qquad (3)$$

Figure 4. Area of the simple fall. A = area of the simple fall, B = base blade area, C = specimen area.

d) Mean length between peaks, *FaPR* (Stylios & Zhu, 1997). This is the arithmetic mean of peak lengths or radii as measured from the specimen centre in mm (see Figure 2). *FaPR*, which can range from 90 to 150 mm, is calculated from the following expression:

$$FaPR = \sum_{i=1}^{n} \frac{FPRi}{n} \qquad (4)$$

e) Mean valley length, *VaFR* (Stylios & Zhu, 1997). Similarly to *FaPR*, *VaFR* denotes the arithmetic mean of valley lengths or radii as measured from the specimen centre in mm (see Figure 2). *VaFR*, which can also range from 90 to 150 mm, is mathematically defined as follows:

$$VaFR = \sum_{i=1}^{n} \frac{VFRi}{n} \qquad (5)$$

f) Peak drape angle, *αFPR* (Stylios & Zhu, 1997). This is the angle between the tangent to the specimen at each peak and its normal (*αFPR*) (see Figure 5). It is expressed in degrees (º) and can range from 0 to 90º. This indicator, which gives a measure of drape intensity, is calculated from the following equation:
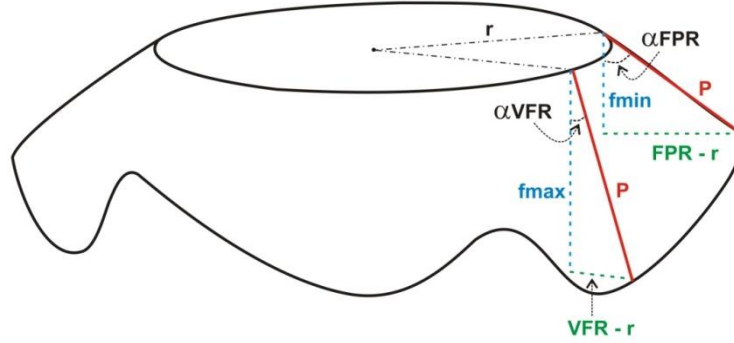
$$aFPR = sen^{-1}\left(\frac{FPR-r}{P}\right) \qquad (6)$$

Figure 5. Elements used to calculate the drape angle for peaks and valleys.

g) Valley drape angle, αVFR (Stylios & Zhu, 1997), which is the angle between the tangent to the fabric at each valley and its normal (αVFR) (see Figure 5). αVFR is expressed in degrees (^{0}) and can range from 0 to 90^0. Like the previous indicator, this provides a measure of drape intensity.

$$aVPR = sen^{-1} \left(\frac{VFR - r}{P} \right) \qquad (7)$$

h) Fold peak variance, FPVar (Stylios & Zhu, 1997). This indicator, which accounts for unevenness and asymmetry in the distribution of peaks in a specimen, is calculated as the variance between peak radii in the specimen:

$$FPvar = \frac{1}{n-1} \sum_{i=1}^{n} \left[FPRi - \left(\frac{1}{n} \sum FPRi \right) \right]^2 \qquad (8)$$

i) Average radius, Ravg (Jeong, 1998). Ravg is the arithmetic mean of drape ratios (i.e., the distance from the specimen centre to the end of the dropped fabric). In this work, it was determined at 0.5^0 intervals and hence as the arithmetic mean of 720 measurements. Ravg is measured in mm and can range from 90 to 150 mm.

$$Ravg = \frac{\sum_{I=1}^{720} Ri}{n} \qquad (9)$$

j) Percent radial distance ratio, %DDR (Jeong, 1998). This indicator is obtained as the ratio of the difference between the radius of the undropped specimen and the average radius to the difference between the radius of the undropped specimen and that of the support disc (see Figure 2). The difference in the numerator coincides with that between the radius of the original specimen and the average radius of the drape profile for the dropped specimen, so the smaller it is, the less deformation the fabric will undergo.

$$DDR\% = \left(\frac{R - Ravg}{R - r}\right) \cdot 100 \qquad (10)$$

k) Fold depth index, *FDI De* (Stylios & Wan,1999). This index is expressed in mm and calculated as the ratio of the difference between mean peak and valley lengths to the difference between the radius of the undropped specimen and that of the support disc:

$$FDI\ De = \frac{FaPR - VaPR}{R - r} \qquad (11)$$

l) Radius variance, *VRi* (Stylios & Wan,1999). This self-developed indicator, which arose from an original proposal elsewhere, is calculated by determining the variance of 720 measurements of the specimen radius at 0.5^{0} intervals. *VRi* is a measure of variability in drape shape.

$$VRi = \frac{1}{n-1} \sum_{i=1}^{720} \left[Ri - \left(\frac{1}{n}\sum Ri\right)\right]^2 \qquad (12)$$

m) Circularity, *CIRC* (Robson & Long, 2000). Circularity is calculated from the equation below, where *Ao* is the area of the shadow cast by the specimen and *P* its perimeter. *CIRC* can range from 0 to 1, with 1 corresponding to a perfect circle (i.e., zero drape) and near-zero values to complex drape profiles. *CIRC* is calculated as the ratio of projected areas, where the area in the numerator is obtained as a function of the particular meter used and that in the denominator from the perimeter of the drape profile. Therefore, this procedure considers fold shape (the larger the perimeter is, the greater in number and/or depth will be the folds).

$$P = 2\pi r \ , \ \ r = \frac{P}{2\pi},$$

$$Ao = \pi \cdot r^2 = \pi \left(\frac{P}{2\pi}\right)^2 = \frac{p^2}{4\pi}$$

$$CIRC = \frac{Ao}{\frac{P^2}{4\pi}} = 4\pi \frac{Ao}{P^2} \qquad (13)$$

n) Mean node severity, *MNS* (Robson & Long, 2000). *MNS* is determined by transforming the drape fold profile on a coordinate system where radii, in mm, are represented on the *y*-axis and angles (or the perimeter of the undropped specimen) on the *x*-axis. *MNS* (mm) is the arithmetic mean of the ratio of fold height (*H*) to width (*W*) (see Figure 6). This indicator is similar to the shape factor but is calculated in a much more realistic manner.
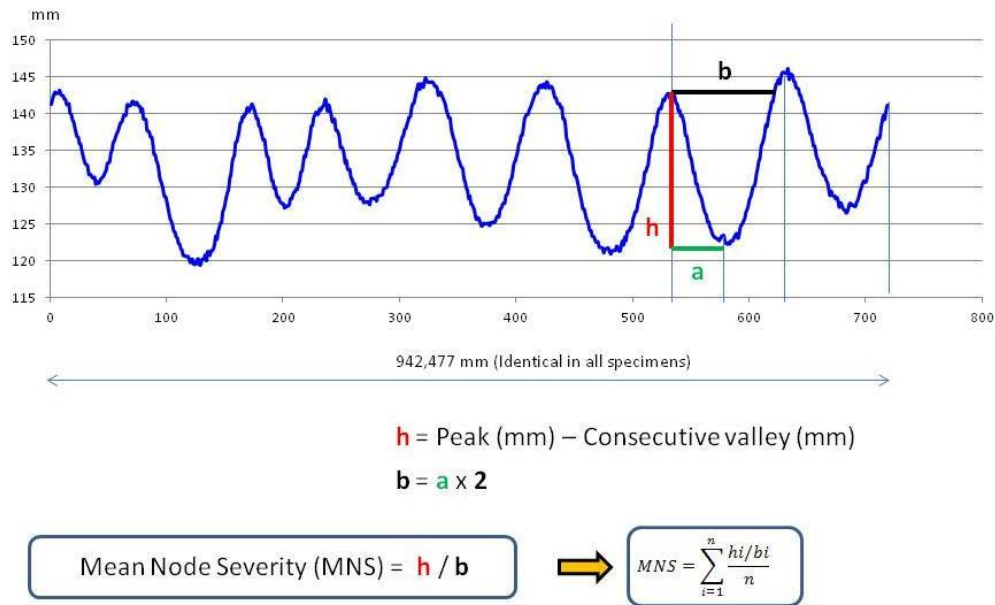
h = Peak (mm) − Consecutive valley (mm)

b = a x 2

Mean Node Severity (MNS) = h / b ⟹ $MNS = \sum_{i=1}^{n} \frac{hi/bi}{n}$

Figure 6. Mean node severity

o) Variability of node severity, *VS* (Robson & Long, 2000). *VS* represents the standard deviation of node severity in a given specimen and is a measure of unevenness in fold shape and severity. This indicator accounts for fold evenness in a specimen but not for fold shape (see Figure 6).

$$VS = \sqrt{\frac{\sum_{i=1}^{n}(MNSi - \overline{MNS})^2}{n-1}} \qquad (14)$$

p) Mean fold width, *FW* (May-Plumlee, Eischen, Kenkare & Pandurangan, 2003), in mm, between adjacent valleys (see Figure 2). The greater *FW* is, the smaller are drape and the number of folds in a specimen.

$$FW = \sum_{i=1}^{n} \frac{FWi}{n} \qquad (15)$$

q) Mean fold height, *FH* (May-Plumlee, Eischen, Kenkare & Pandurangan, 2003), measured, in mm, from the line used to measure *FW* (see Figure 2).

$$FH = \sum_{i=1}^{n} \frac{FHi}{n} \qquad (16)$$

r) Fold distribution, %*Gp* (Jevsnik & Gersak, 2004). *%Gp* represents the percent coefficient of variation of peak length (*FPR*, Figure 2) and is a measure of variability in fold shape and symmetry in each specimen.

$$Gp\% = \frac{\sqrt{\frac{\sum_{i=1}^{n}(FPRi - \overline{FPR})^2}{n-1}}}{\overline{FPR}} \cdot 100 \qquad (17)$$

s) Mean fold depth, *dga* (Jevsnik & Gersak, 2004), which is the difference between the mean peak length and valley length, in mm. The greater the difference is, the greater is fold depth —and hence the visual appearance of drape severity— in a specimen.

$$dga = FaPR - VaFR \qquad (18)$$

t) Maximum drape, *fmax* (Jevsnik & Gersak, 2004), which is given by the sine of the valley drape angle *(αVFR*, Figure 5):

$$fmax = \sqrt[2]{(R-r)^2 - (r-VaFR)^2} \qquad (19)$$

u) Minimum drape, *fmin* (Jevsnik & Gersak, 2004), which is calculated as the sine of the peak drape angle (*αFPR*, Figure 5).

$$fmin = \sqrt[2]{(R-r)^2 - (r-FaPR)^2} \qquad (20)$$

v) Dominant wavelength amplitude, *WA* (Park, Kim, 2004). In 1807, Fourier found that any periodic signal can be represented by a sum of harmonically related trigonometric (sine and cosine) terms. So-called "Fourier transform" (*FFT*) is the frequency spectrum for a function converging on a continuous periodic function that can be split into an infinite sum of much more simple sine functions. The transform includes a dominant sine function and several secondary functions the combination of which yields the initial function. The *WA* indicator introduced a paradigmatic change in the way fabric drape was assessed by assuming it to be a periodic function that can be converted into a Fourier series. This mathematical tools provides the dominant wave frequency. Making 720 radius readings (2 per degree) of the shadow cast by a dropped specimen allowed us to represent the drape profile on a Cartesian plane with radii on the *y*-axis and angles (0–360º) on the *x*-axis. This information was used to calculate the corresponding Fourier transform with the aid of the software MATLAB, and also the dominant wavelength (mm).

v) Fitness factor, *D/O* (Park, Kim & Yu, 2004). In line with the previous one, this self-developed indicator is calculated as the ratio of the areas bound by the curve of the dominant wave in the Fourier transform to that of the original shadow cast by the specimen. If the ratio is near-unity, the original curve is very similar to the curve of the dominant wave, which is a perfect sine function. As a result, the original curve will result in a highly even, symmetric drape with very similar shapes (i.e., a high periodicity and evenness). In fact, *D/O* accounts for shape evenness and symmetry —and hence for geometric isotropy. The more *D/O* departs from 1, the less isotropic —or more anisotropic— will be drape shape. This indicator can range from 0 (minimum geometric isotropy) to 1 (maximum geometric isotropy).

w) Equivalent circle radius, *ecr* (Mizutani, Amano & Sakaguchi, 2005). This is the radius of an equivalent circle having the same area as the drape shadow, in mm, which can range from 90 to 150 mm (see Figure 2).

$$ecr = \sqrt[2]{A/\pi} \qquad (21)$$

x) Mean radius amplitude, *A/r* (Mizutani, Amano & Sakaguchi, 2005). *A/r* is the ratio, in mm, of the mean fold amplitude to the radius of an imaginary circle having the same area as the drape shadow (ecr, Figure 2). When ecr is similar to the specimen radius, the fabric undergoes little deformation and fold amplitude is small; as a result, *A/r* is high. Conversely, the greater is *r*, the less the fabric deforms, the smaller is fold amplitude and the lower is *A/r*.

$$\frac{A}{r} = \frac{\frac{dga}{2}}{rce} \qquad (22)$$

y) *R factor* (Mizutani, Amano & Sakaguchi, 2005). This indicator, expressed in mm, is a measure of drape simplicity.

$$R\ factor = \frac{\sqrt[2]{\overline{(r\iota - rce)^2}}}{rce - R} \qquad (23)$$

where $\overline{(r\iota - ecr)^2}$ is the average value of $(ri - rce)^2$ along the contour of the drape profile; r_i, *ecr* and *R* denote the radial coordinates of drape shadow, equivalent circle radius and specimen radius, respectively. The *R factor* is a measure of drape simplicity or unevenness; the greater it is, the less simple will be drape shape.

z) Angle between consecutive folds, α (Jevsnik & Zunic-Lojen, 2007). This indicator, expressed in degrees, is calculated as the arithmetic mean of the angle between consecutive folds in a specimen. Such an angle can vary widely in the same specimen depending on its degree of asymmetry. However, the arithmetic mean of the angle throughout a specimen offsets the differences and is very close to the ratio of 360º to the number of folds in the specimen. This shortcoming detracts from the interest of this indicator.

$$\alpha = \sum_{i=1}^{n} \frac{\alpha i}{n} \qquad (24)$$

aa) Percent fold depth, *%FDI De* (Behera & Pattanayak, 2008), which is calculated as the ratio of fold depth to the difference between the specimen radius and support disc radius multiplied by 100:

$$\%FDI\ De = \left(\frac{dga}{R-r}\right) \cdot 100 \qquad (25)$$

bb) Radius half-amplitude, *ARR* (Behera & Pattanayak, 2008), which is calculated as one-half the mean fold depth and expressed in mm.

$$ARR = \frac{dga}{2} \qquad (26)$$

cc) Fractal dimension, *D* (Payvandy, 2011). The fractal dimension of the drape profile is calculated by using the Box-counting method, which involves scaling a square or cube of 1 cm dimension by a factor ε and spanning the resulting geometric figures with $N(\varepsilon)$ similar figures in accordance with the following power law:

$$N(\varepsilon) = \left(\frac{1}{\varepsilon}\right)^{D} \qquad (27)$$

where exponent *D* is the number of figure dimensions (1 for a segment, 2 for a square and 3 for a cube). Therefore, the dimensions of the classic geometric figures are all whole numbers.

The previous law can be applied to figures with auto-similar structures (i.e., figures formed by repeating an architectural pattern), which therefore have an identical representation even when upscaled or downscaled. Such figures are called "fractals" and have coefficient *D* as their dimension. *D* is given by the following power law:

$$D = \frac{\ln N(\varepsilon)}{\ln\left(\frac{1}{\varepsilon}\right)} \qquad (28)$$

The fractal dimension is a decimal number. Because they fall between two whole numbers, fractals cannot be dealt with as "normal" shapes. Also, natural fractals are strictly not auto-similar and their power laws hold with very small ε values only:

$$D = \lim_{\varepsilon \to 0} \left(\frac{\ln N(\varepsilon)}{\ln\left(\frac{1}{\varepsilon}\right)}\right) \qquad (29)$$

The fractal dimension is typically estimated by using the Box-counting method (23), which involves superimposing a figure onto a grid of cell length ε and counting the number of cells spanned by the original figure; the counting process is then repeated with other cell sizes (ε). The slope of a plot of $\ln N(\varepsilon)$ vs $\ln\left(\frac{1}{\varepsilon}\right)$ provides *D*:

$$\ln N(\varepsilon) = \ln k + D \cdot \ln\left(\frac{1}{\varepsilon}\right) \qquad (30)$$

There are other, alternative dimensions including the correlation dimension —which, together with the Box-counting dimension are the most widely used by virtue of their easy calculation—, the Hausdorff dimension —the most important in theoretical terms—, the Rényi dimension and the information dimension. In order to avoid confusion, the Box-counting fractal dimension is usually denoted by D_C —in this paper, however, we have omitted the subscript because the only fractal dimension used is the Box-counting dimension.

dd) Drape unevenness, *DU%* (Al-Gaadi, Göktepe & Halász, 2012), which is the coefficient of variation between consecutive folds and accounts for drape symmetry in each specimen but not for drape shape. This indicator is expressed as a percentage and can range from 0% (maximum symmetry) to 100% (minimum symmetry).

$$DU\% = \frac{\sqrt{\frac{\sum_{i=1}^{n}(\alpha i - \bar{\alpha})^2}{n-1}}}{\bar{\alpha}}\ 100 \qquad (31)$$

ee) Fold height, *H* (Al-Gaadi, Göktepe & Halász, 2012)), which is calculated as one-half the combined mean peak and valley length, in mm:

$$H = \frac{FaPR + VaPR}{2} \qquad (32)$$

ff) Amplitude, *WAM* (Al-Gaadi, Göktepe & Halász, 2012). This is the ratio of *ARR* (radius half-amplitude) to *H* (fold height), expressed in mm:

$$WAM = \frac{ARR}{H} \qquad (33)$$

gg) Height-to-angle ratio, *R H/α* (Al-Gaadi, Göktepe & Halász, 2012), which is calculated as the ratio of fold height to fold angle and represents the length of drape profile spanning an angle of 1º:

$$R\ H/\alpha = \frac{H}{\alpha} \qquad (34)$$

hh) Area/perimeter ratio, *A/P* (Al-Gaadi, Göktepe & Halász, 2012), which is calculated as the ratio of drape area to perimeter:

$$\frac{A}{P} = \frac{Area\ under\ drape\ shadow}{Perimeter\ of\ drape\ profile} \qquad (35)$$

ii) Fold profile, *Fsp* (self-developed). Fsp (mm), which represents the difference between fold width and height, is an easily determined measure of fold shape and severity.

$$Fsp = FW - FH \qquad (36)$$

Each drape indicator reported to date is based on a specific approach to the examination, description, assessment or simulation of drape. Overall, however, drape indicators can be classified conceptually into five different categories, namely:

(a) *Area and perimeter based measures*. Drape is calculated from the area of the shadow cast by a specimen, which is either measured directly or estimated from the equivalent circle corresponding to the radius and/or perimetral length of the area.

(b) *Radius based measures.* Drape is determined by measuring the radii of different sections of the drape shadow (e.g. the mean radius, the radius of the equivalent circumference, the radial distance ratio or its variance). These measures provide estimates of circularity or regularity in drape shape.

(c) *Node based measures.* Drape is calculated from some node property such as number, depth, a dimension (width, height), distribution or regularity.

(d) *Profile based measures.* These assess some characteristic of the drape profile (severity, slimness, symmetry) as determined by using appropriate mathematical tools such as Fourier series or fractals.

(e) *Three-dimensionally simulated measures.* The interest of designers and graphical computation researchers in simulating fabric drape three-dimensionally has led to the development of tools for measuring specific drape geometry parameters such as drape angle to facilitate the three-dimensional interpretation of drape.

Objectives

The drape ratio (*%DR*) provides an objective, albeit incomplete description of fabric drape. Thus, a fabric with a low ratio is easily deformed and has a high drape, and the opposite holds for one with a high ratio (see Fig. 7).
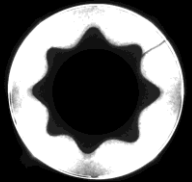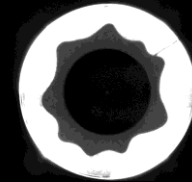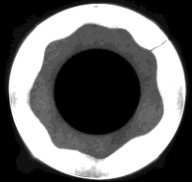

| *%DR* | 25.072 | 45.013 | 55.900 | 73.334 |

Figure 7. Appearance of the drape profile for four fabrics differing in drape ratio (*%DR*).

However, the drape ratio cannot explain the complex three-dimensional structure of drape; in fact, two fabrics with an identical ratio can have a markedly different drape shape (see Fig. 3).
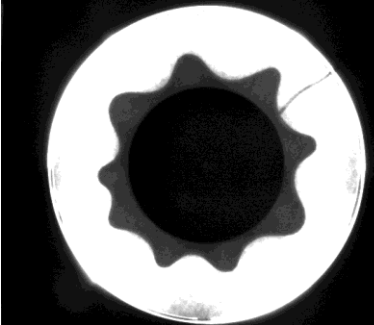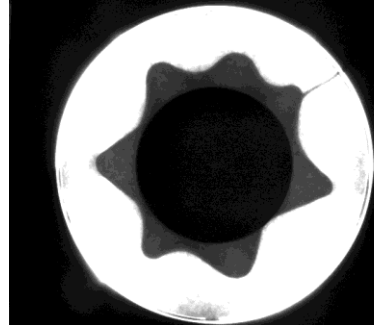
Ref.	A	B
Image		
%DR	39.518	39.698
FN	9	7

Figure 8. Two fabrics with the same drape ratio can differ in drape profile.

This work was undertaken with three well-defined objectives, namely:

(a) To conduct a literature search for major drape indicators reported since 1950 and examine their contribution to the accurate characterization of such a complex phenomenon as fabric drape.

(b) To select a small number of effective, mutually independent (i.e. not strongly correlated) indicators with a view to assessing and explaining drape.

(c) Since two fabrics can differ markedly in drape profile shape but have an identical drape ratio, we sought to identify individual indicators or combinations thereof allowing such fabrics to be discriminated in terms of drape shape.

Methodology

A literature search allowed us to identify a total of 36 drape indicators that were then determined in 37 different commercial woolmaking, clothmaking, shirtmaking and lining woven fabrics spanning a wide range of composition, aerial weight (50–447 g/m^2), weave type and density (see Table 1).

Composition (%)	Weave type	Aerial weight (g/m^2)	Ref.
WO/PAN 60/40	Double cloth	447.41	1
PES/CV/EA 64/31/5	Double cloth	371.45	2
PES/CV/EA 78/18/4	Serge	341.33	3
WO/PA 90/10	Double cloth	333.26	4
CO/WO/PA 76/19/5	Two-sided cloth	309.14	5
WO 100%	Satin	299.41	6
PES/CV/EA 78/17/5	Serge	279.08	7
CO 100%	Basket	241.16	8
WO/EA 99/1	Crepe	232.16	9
PES/CV/EA 65/31/4	Taffeta	221.17	10
CO 100%	Herring bone	214	11
WO 100%	Serge	209	12
WO/PES 60/40	Herring bone	199.08	13
WO 100%	Serge	191.08	14
LI 100%	Taffeta	186.9	15
PES 100%	Taffeta	172.622	16
CV/WO/PES 43/34/24	Taffeta	171.25	17
CO 100%	Serge	169.5	18
PES/LI 55/45	Serge	163.58	19
WO/LI/CO/PA 36/32/16/16	Serge	157.71	20
CO/PES 65/35	Herring bone	135.17	21
CO/LI 43/57	Taffeta	100	22
CO/PES 65/35	Taffeta	90	23
PES 100%	Satin	90	24
PES/CV 60/40	Satin	90	25
CV/CA 55/45	Serge	80	26
PES 100%	Satin	78.4	27
CV/PES 50/50	Jacquard	77.5	28
PES 100%	Serge	76.5	29
CV 100%	Serge	72	30
CV 100%	Taffeta	70	31
CV/PES 60/40	Serge	70	32
CV/PES 60/40	Serge	68.5	33
CA 100%	Taffeta	68	34
PES/CV 50/50	Taffeta	65	35
PES/CV 50/50	Serge	65	36
PES 100%	Taffeta	50	37

Table 1. Composition, weave type and aerial weight of the studied fabrics.

Tests were conducted at the Textile Physics Laboratory of the Department of Textile and Paper Engineering of the Polytechnical University of Catalonia (UPC), using a Cusick drape meter equipped with a CCD digital camera mounted at the top (see Fig. 9).
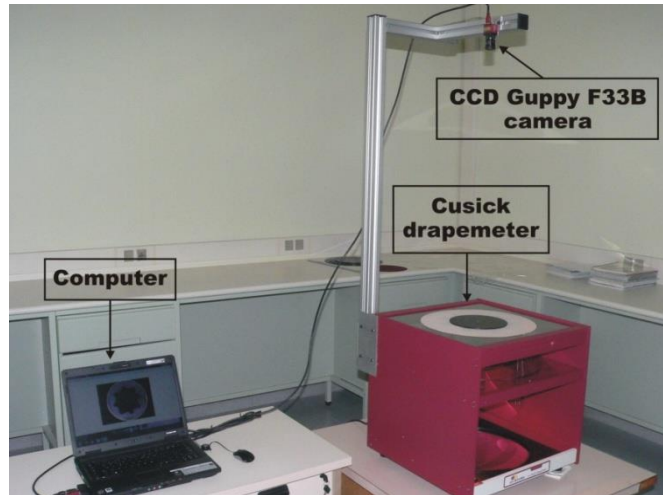
Figure 9. UPC digital drape meter of the Textile Physics Laboratory of the Department of Textile and Paper Engineering of the Polytechnical University of Catalonia (UPC).

The camera was calibrated to measure the number of pixels per square centimetre spanned by the captured images, and to correct optical and alignment distortions prior to performing various geometric calculations with the imaging software Sherlock[TM]. Greyscale digital photographs of drape shadow were converted into monochrome (binary) images by filtering threshold noise and the filtered images were processed with Sherlock[TM] to calculate the target geometric parameters listed in Table 2 (see also Figs 2–6).

Parameter	Units
Specimen projected area, A	mm^2
Fold Number, FN	n
Fold Peak Radius,. FPR	mm
Average Fold Peak Radius, F_aPR	mm
Valley Fold radius, VFR	mm
Average Valley Fold radius, V_aFR	mm
Fold Width, FW	mm
Fold Height, FH	mm
Angle between Consecutive Folds, α	(º)
Radii (720), R_i Distance from specimen centre to edge of dropped fabric shadow as determined at 0.5º intervals (i.e., with 720 measurements)	mm
Perimetral length of the specimen shadow, P	mm

Table 2. Parameters of drape geometry as determined with the software Sherlock[TM]

A total of 4 randomly selected specimens of each fabric were used. Each specimen was 300 mm in diameter. Also, as set by the standard for this test (BS 5058), the support disc was 180 in diameter.

Each specimen was subjected to 3 tests at different rotation angles (0º, 90º and 135º) in order to ensure that the results would not be affected by specimen position, both on the face and on the reverse; therefore, each result was the arithmetic mean of 24 measurements. The average radius, R_{avg}, was calculated as the arithmetic mean of 720 measurements at a 0.5º rotation interval of the distance from the specimen centre

to the edge on each side of the fabric. The final result was the average of the 24 arithmetic means.

All tests were performed on specimens conditioned in a standard atmosphere.

Correlation between drape ratio as determined with the Cusick meter (i.e. by cutting and weighing the paper area containing each drape projection) and with the UPC digital drape meter (i.e. from the number of pixels spanned by the drape area) was found to be very high (Pearson's correlation coefficient = 0.997, $p = 0.000$).

Factor analysis and cluster analysis

The general designations "factor analysis" and "cluster analysis" encompass various multivariate analysis techniques that are used to examine relationships between variables. Both are intended to facilitate grouping of variables, which in this work was accomplished by using a correlation matrix. In factor analysis, variables are grouped in terms of the variability with other, not directly observable variables (common factors); by contrast, cluster analysis groups variables in terms of nearness or similarity. Both rely on the principles of parsimonious analysis (i.e., they seek the most simple possible data structure representing homogeneous groups) and interpretability (i.e., the resulting groups must possess practical significance).

In this work, the underlying structure of data was elucidated by factor analysis. This was followed by graphical examination of the dendrogram obtained by cluster analysis —in fact, classification is a fundamental scientific process because phenomena must be sorted before they can be understood.

In factor analysis, each observed variable is expressed as a linear combination of a small number of common latent factors and an error term. The model can be represented by the following algebraic equation:

$$x = A \cdot f + e \qquad (37)$$

where

$$A = \begin{bmatrix} a_{11} & \cdots & a_{1k} \\ \cdots & \cdots & \cdots \\ a_{pl} & \cdots & a_{pk} \end{bmatrix}, f = \begin{bmatrix} f_1 \\ \cdots \\ f_k \end{bmatrix}, e = \begin{bmatrix} e_1 \\ \cdots \\ e_k \end{bmatrix} \qquad (38)$$

a_{ij} being the factor weights expressing the dependence of each variable x_i on the common factors f_i and used to interpret the factors. Thus, a high a value for a factor allows the factor to be associated with a specific variable and hence to be characterized.

The number of factors used coincides with that of principal components (i.e., of linear combinations of the original variables) extracted —by maximizing the variance of the components— from the variables and each principal component accounts for a fraction of the overall variance. The coefficient of correlation (factor weight) between each component and variable is calculated by multiplying the weight of the variable in that component by the square root of its eigenvalue.

The data examined in this work were drape indicator values. Based on the size of our sample, we chose to use an ascending hierarchical clustering method. The process

uses as many clusters as variables are to be classified. Then, the two variables exhibiting the greatest closeness or similarity are combined. In the third step, a new cluster is established by combining two other variables or adding a third to the previous pair. Clusters are thus formed in a gradual, ascending manner. The process is finished when a single cluster containing all variables is obtained.

The similarity measure used here was Pearson's correlation coefficient. In this context, the coefficient between two variables x_i and x_j was defined as follows:

$$r_{ij} = \frac{\sum_{k=1}^{n}\left(x_{ik} - \overline{x}_i\right)\left(x_{jk} - \overline{x}_j\right)}{\sqrt{\sum_{k=1}^{n}\left(x_{ik} - \overline{x}_i\right)^2 \sum_{k=1}^{n}\left(x_{jk} - \overline{x}_j\right)^2}} \qquad (39)$$

We used the absolute value of each correlation since the aim was to assess the "strength" of relationships between variables rather than identify their "direction".

Variables were hierarchically clustered by using various classification algorithms; because all led to the same clusters, we selected the "nearest neighbour" or "complete-linkage" algorithm. With this algorithm, the similarity s between a cluster $(x_i + x_j)$ and an unclassified variable x_k is given by the minimum of the variables in the cluster to the new variable:

$$s\left[x_k\left\{x_i + x_j\right\}\right] = \min\left[s\left(x_k x_i\right), s\left(x_k x_j\right)\right] \quad (40)$$

Results and discussion

The 36 above-described drape indicators were calculated for the 37 woven fabrics studied. The results were used to construct a correlation matrix containing 630 values. Many of the indicators exhibited a high correlation with drape ratio by effect as a result of the geometric relationship between them; therefore, such indicators were useless with a view to circumventing the shortcomings of *%DR* in determining drape shape and excluded from the study.

In a subsequent step, we additionally excluded redundant indicators, namely:

(a) R_{avg} which was identical with *ecr* and more difficult to calculate.

(b) αFPR and αVFR because they were derived from *FaPR* and *VaFR*, respectively.

(c) *ARR* because it was simply an arithmetic transformation of *dga*.

(d) *%FDI De* because it was obtained by converting the dimensions used to express *FDI De*.

(e) *FDI De* because it was equivalent to *dga*.

(f) *WAM* because it was identical with *A/r* but more complicated to calculate.

We then discarded those indicators with correlation coefficients exceeding 0.80 (Berry, & Feldman,1985) (Hutcheson & Sofroniu,1994) in order to avoid multicollinearity. As a result, the initial set of 36 indicators was reduced to 7 whose correlation matrix shown in Table 3.

FN	FH	%DU	%Gp	VS	D/O	
−0.706	−0.084	0.186	−0.249	−0.170	0.547	**%DR**
	−0.607	−0.037	0.028	0.210	−0.292	**FN**
		−0.156	0.154	0.462	−0.236	**FH**
			0.589	0.060	−0.043	**%DU**
				0.150	−0.526	**%Gp**
					−0.135	**VS**

Table 3. Correlation matrix for the indicators with a correlation coefficient equal to or less than 0.80.

The purpose of the factor analysis was to obtain a small number of factors accounting for most of the variability in the seven variables examined. As can be seen from Table 4, only three factors among the seven had an eigenvalue greater than or equal to 1.0 and were thus selected. In combination, the three factors accounted for 82.618 % of variability in the original data. Since we chose to use principal component analysis, initial communality estimates were set under the assumption that the whole variability in the data was due to common factors.

Factor	Eigenvalue	Variance (%)	Cumulative variance (%)
1	2.339	33.416	33.416
2	1.974	28.213	61.628
3	1,469	20.991	82.619
4	0.671	9.592	92.211
5	0.398	5.697	97.909
6	0.125	1.790	99.699
7	0.021	0.301	100.000

Table 4. Results of the factor analysis

Table 5 shows the factor loadings for the common factors after Varimax rotation. Rotation was used to simplify the explanation of each factor. The table also shows the estimated communalities, which were used as estimates of percent variability in each variable due to the extracted factors. The asterisks in the table denote the factors saturating the indicators. Clearly, the first factor was represented by *%DR* and *FN*; the second by *%DU*, *%Gp* and *DO*; and the third by *FH* and *VS*.

Indicator	Factor 1	Factor 2	Factor 3	Estimated communality	Specific variance
%DR	0.967 *	−0.020	−0.154	0.961	0.038
FN	−0.822*	−0.003	−0.533	0.961	0.038
FH	0.085	0.001	0.932 *	0.877	0.122
%DU	0.190	0.911 *	−0.157	0.892	0.107
%Gp	−0.172	0.840 *	0.174	0.767	0.232
VS	−0.089	0.083	0.734 *	0.553	0.446
DO	0.571	−0.621 *	.−0.241	0.770	0.229

Table 5. Factor loading matrix after Varimax rotation

The three factors were easily calculated from the standard indicators used in the analysis:

$$f_1 = 0.502\ \%DR - 0.401\ FN + 0.006\ FH + 0.194\ \%DU - 0.013\ \%Gp - 0.068\ VS + 0.242\ D/O \quad (41)$$
$$f_2 = -0.094\ \%DR + 0.044\ FN + 0.056\ FH - 0.526\ \%DU - 0.428\ \%Gp - 0.016\ VS + 0.265\ D/O \quad (42)$$
$$f_3 = -0.125\ \%DR - 0.263\ FN + 0.516\ FH - 0.161\ \%DU + 0.045\ \%Gp + 0.407\ VS - 0.114\ D/O \quad (43)$$

Cluster analysis of the data of Table 3 allowed the classification tree (dendrogram) of Figure 10 to be constructed in order to graphically monitor the variable combination process, identify combined groups, and assess their combination level and similarity.

Drawing a horizontal line at a reasonably long distance (e.g. a similarity level of 37.18) allowed the following indicator clusters, which coincided with common underlying factors in the data structure, to be established:

   (a) Cluster 1 *(%DR* and *FN)*.

   (b) Cluster 2 (*FH* and *VS*).

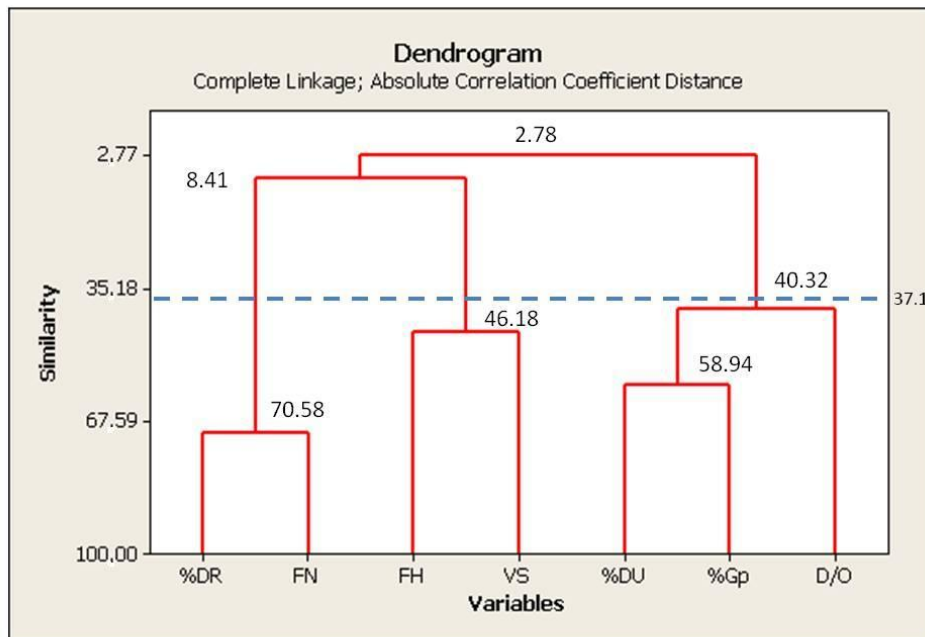   (c) Cluster 3 *(%DU, %Gp* and *FF D/O)*.

Figure 10. Complete-linkage dendrogram for the 7 selected indicators

The first cluster explained drape intensity: the lower *%DR* was, the higher was drape (see Fig. 7); also, the greater *FN*, the greater the visual sensation of drape —this indicator, however, failed to completely account for drape shape (see Fig. 8).

The second cluster partly explained drape shape (i.e. the severity or depth of *FH* nodes) and hence roughness (the greater *FH*, the lesser the roughness, Fig. 11) and regularity in *VS* (Fig. 12).
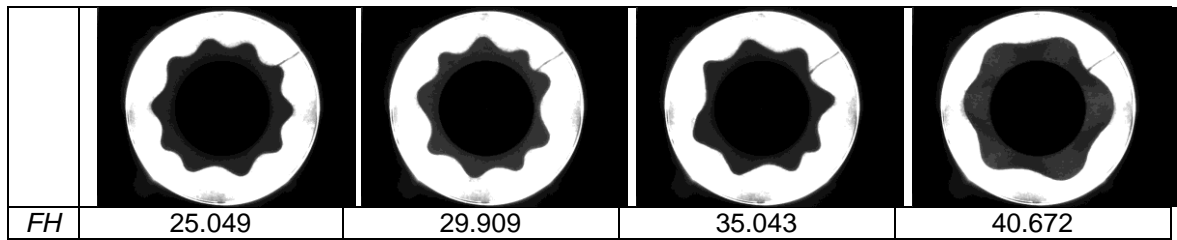
| FH | 25.049 | 29.909 | 35.043 | 40.672 |

Figure 11. Variation of drape profile with *FH*.
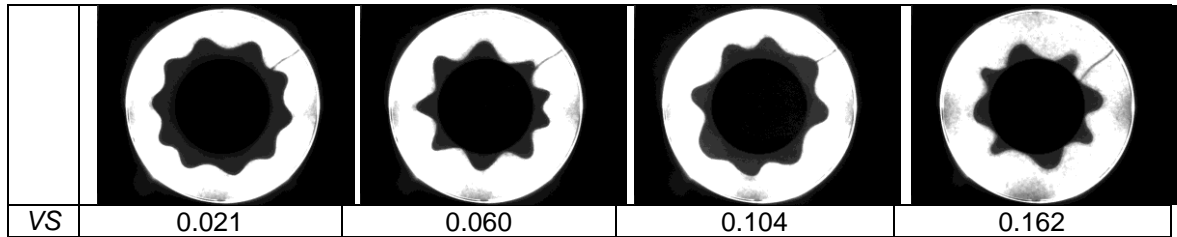

| VS | 0.021 | 0.060 | 0.104 | 0.162 |

Figure 12. Variation of drape profile with *VS*.

The third cluster was independent of the previous two and explained both geometric isometry (the lower *%DU* or the higher *D/O*, the higher the symmetry, Figs 13 and 14) and irregularity in the drape profile (the higher *%Gp*, the greater the difference in length between specimen peaks, Fig. 15).
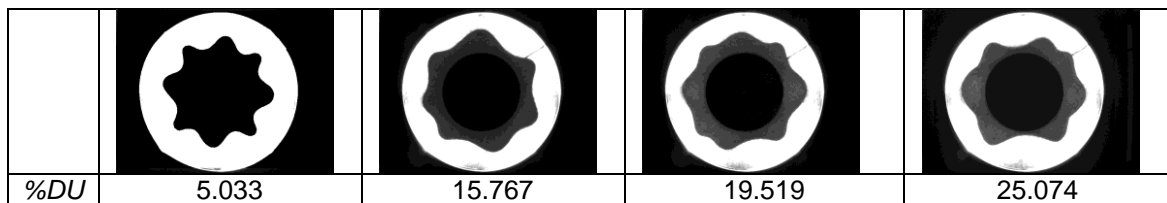

| %DU | 5.033 | 15.767 | 19.519 | 25.074 |

Figure 13. Variation of drape profile with *%DU*.

| D/O | 0.950 | 0.970 | 0.981 | 0.999 |
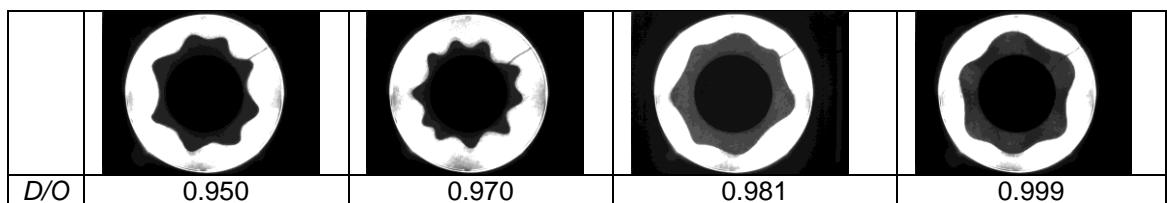
Figure 14. Variation of drape profile with *D/O.*

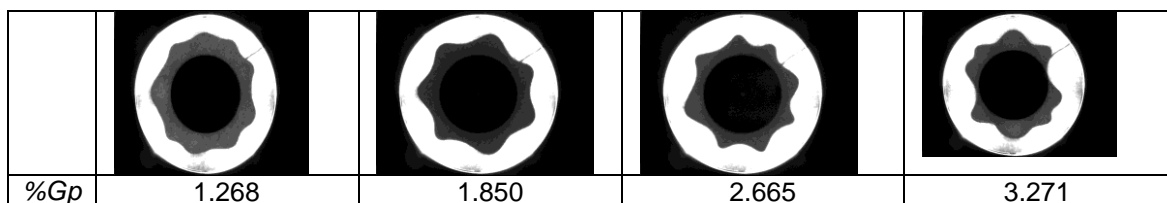| %Gp | 1.268 | 1.850 | 2.665 | 3.271 |

Figure 15. Variation of drape profile with *%Gp.*

Hierarchical clustering methods impose a specific structure on data and can introduce severe distortions in the original relations. In order to confirm whether this was the case with our results, we calculated the cophenetic correlation coefficient (viz. correlation between the values in the original similarity matrix and those in the so-called "cophenetic matrix", which contained the values defining similarity between indicators included in a given cluster). The coefficient of cophenetic correlation between the similarity values of Table 3 and those of the dendrogram of Fig. 10 was 0.74 —the coefficient for two identical matrices is unity. Therefore, the distortion introduced by the clustering method was acceptable.

Finally, we assessed the usefulness of the seven indicators for discriminating the 37 fabrics studied in terms of drape shape and found the following criterion to be met in all instances: fabrics with an identical drape ratio thus have to be distinguished by the number of nodes (FN): the greater *FN* is, the greater will be the visual sensation of drape (Fig. 16).
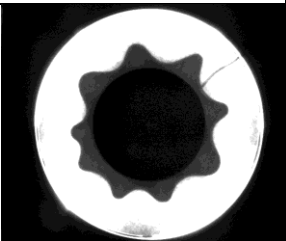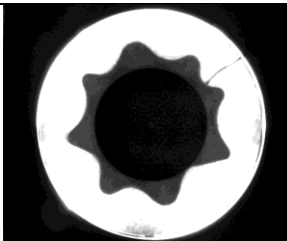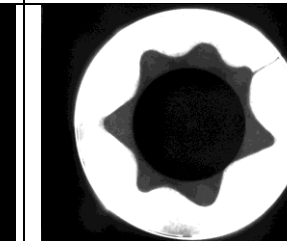
Ref	A	C	B
%DR	39.518	39.893	39.698
FN	9	8	7

Figure 16. Drape profiles for three fabrics with the same *%DR* and a different *FN* value.

On equal *%DR* and *FN*, *FH* can be used to predict severity (sharper nodes) or roughness (node depth) in the drape profile since roughness increases with increasing *FH* (Fig. 17).
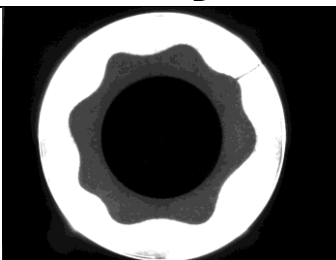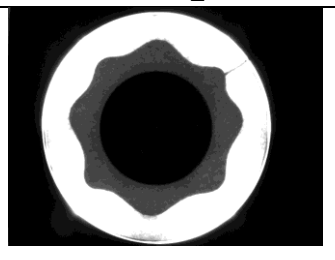
Ref.	D	E
Image		
%DR	64.934	64.815
FN	8	8
FH	29.208	27.934

Figure 17. Drape profiles for two fabrics with the same *%DR* and *FN* but a different *FH* value.

In those cases where *%DR*, *FN* and *FH* provide essentially indistinguishable results, *%DU* is the best choice for discriminating symmetry and regularity in the distribution of nodes in the drape profile (Fig. 18).
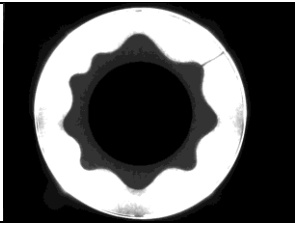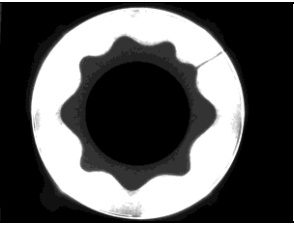
Ref	H	I
Image		
%DR	51.772	51.820
FN	9	9
FH	28.587	28.611
VS	0.0761	0.0605
%DU	17.831	15.722
%Gp	2.506	1.966
D/O	0.9850	0.9839

Figure 18. Drape profiles for two fabrics with the same %DR, FN and FH but a different %DU value.

The indicator *VS* is complementary with *FH*, but not as sensitive to differences in drape shape. *%Gp* is a useful complement for *%DU* as it accounts for unevenness in peak dimensions. Finally, *D/O* is a complement for *VS* and *%Gp* but need not be determined since these two suffice to discriminate between drape shapes. In summary, sequentially determining four indicators (viz., *%DR, FN, FH* and *%DU*) allows drape profiles to be fully characterized in terms of intensity, roughness and geometric isotropy. This sequential four-indicator criterion was used to experimentally validate 15 additional woven fabrics (see Table 6). The indicators accurately explained differences in drape profile between fabrics.

Composition	Weave type	Aerial weight (g/m^2)	Ref.
WO 100%	Serge	324.95	1
WO/CV	65/35	269.80	2
WO 100 %	Serge	210.90	3
PES/CO 50/50	Taffeta	199.67	4
PES 100%	Serge	195.60	5
PES/CV 65/35	Taffeta	180.23	6
PES 100%	Serge	172.62	7
CO 100%	Taffeta	162.10	8
CV 100 %	Taffeta	161.25	9
WO 100 %	Serge	155.00	10
CV 100%	Taffeta	149.0	11
PES/LI 45/55	Taffeta	100.00	12
PES 100%	Taffeta	81.30	13
PES/CV 50/50	Serge	75.30	14
PES 100%	Taffeta	65.00	15

Table 6. Composition, weave type and aerial weight of 15 fabrics used to validate the sequential indicator criterion used to distinguish drape shape

Conclusions

The mathematical significance of all drape indicators developed by textile researchers from 1968 to 2013 is for the first time described in this paper. Most of the 36 indicators reported to date are highly correlated with drape ratio (*%DR*) by effect of the geometric relationship between the indicators and drape shadow.

Reducing the indicator correlation matrix revealed that only 7 of the 36 indicators studied provided an accurate description of such a complex phenomenon as drape. Such indicators can be classified into three groups according to (a) drape intensity, (b) severity or roughness and (c) shape isotropy and variability.

In the absence of images for visual inspection, fabric drape can be compared by using the following criteria:

(a) The lower is *%DR*, the greater will be drape.

(b) On equal *%DR*, the greater is number of nodes (*FN*) of a fabric, the greater will be its visual sensation of drape.

(c) On equal *%DR* and *FN*, the greater is FH, the more severe and/or rough will be its drape profile.

(d) On equal *%DR*, *FN* and *FH*, the lower is *%DU*, the greater will be geometric isotropy and the smaller irregularity in node distribution.

As shown in this paper, determining four specific drape indicators (viz., *%DR*, *FN*, *FH* and *%DU*) allows drape shape in a woven fabric to be accurately characterized in terms of intensity, roughness and geometric isotropy. This criterion was experimentally validated on 15 additional commercial woven fabrics of variable composition and aerial weight.

References

Al-Gaadi, B. Göktepe, F. & Halász, M. (2012). A new method in fabric drape measurement and analysis of the drape formation process. *Textile Research Journal*, 82: 502-512.

Behera, B. K. & Pattanayak, A. K.(2008). Measurement and modelling of drape using digital Image processing. *Indian Journal of Fibre & Textile Research*, 33, 230-238.

Berry, W.D. & Feldman, S. (1985). *Multiple regression in practice. Series: Quantitative Application in the Social Sciences*. SAGE. Bevery Hills.

Chu, C. C., Cummings, C. L. & Teixeira, N. A. (1950). Mechanics of Elastic Performance of Textile Materials. Part V: A Study of the Factors Affecting the Drape of Fabrics. the Development of a Drape Meter. *Textile Research Journal*, 20, 539-548.

Chu, C.C., Platt, M.M. & Hamburguer, W. (1960). Investigation on the Factors Affecting the Drapeabillity of Fabrics. *Textile Research Journal*, 30,66-67.

Cusick, G. E. (1962). *A Study of Fabric Drape.* University of Manchester.

Cusick, G. E. (1965). The Dependence of Fabric Drape on Bending and Shear Stiffness. *Journal of the Textile Institute*, 56, 596-606.

Cusick, G.E. (1968). The measurement of fabric drape. *Journal of The Textile Institute*, 59, 252-260.

Hutcheson,G. & Sofroniu,N. (1994). *The Multivariate Social Scientist*. SAGE. London.

Jeong, Y. J. (1998). A Study of Fabric-Drape Behaviour with Image Analysis Part I: Measurement, Characterisation, and Instability. *Journal of the Textile Institute*, 89, 59-69.

Jevsnik, S. & Gersak, J. (2004). Modelling the Fused Panel for a Numeric Simulation of Drape. *Fibres & Textiles in Eastern Europe*, 12, 47-52

Jevsnik, S. & Zunic-Lojen, D. (2007). Drape Behaviour of Seamed Fabrics. *Fibers and Polymers*, 8, 550-557.

May-Plumlee, T., Eischen, J., Kenkare,N. & Pandurangan, P. (2003). *Evaluating 3D Drape Simulations: Methods and Metrics.* in *Proceedings of International Textile Design and Engineering Conference (INTEDEC)*, Edinburgh, Scotland.

Mizutani, C., Amano, T. & Sakaguchi, Y. (2005). A New Apparatus for the Study of Fabric Drape. *Textile Research Journal*, 75, 81-87.

Park,C.K., Kim, S. & Yu, W.R. (2004). Quantitative Fabric Drape Evaluation System Using Image Processing Technology (Part 1: Measurement System and Geometric Model). *Journal of Testing Evaluation*, 32, 131-137.

Payvandy, P. (2011). *Evaluation of Fabric Drape Using Image Processing and Fractal Dimension*. MVIP, 2011. The 7th Iranian Conference on Machine Vision and Image Processing. Iran University of Science and Technology.

Robson, D., Long, C. C. (2000). Drape Analysis using Image Techniques. *Clothing and Textiles Research Journal*, 18, 1-8.

Sharma, K.S., Behera,B.K., Roedel,H. & Schenk, A. (2005) Effect of sewing and fusing of interlining on drape behaviour of suiting fabrics. *International Journal of Clothing Science and Technology*. 17, 75-90.

Stylios, G. K. & Zhu, R. (1997). The Characterisation of the Static and Dynamic Drape of Fabrics. *Journal of the Textile Institute*, 88, 465-475.

Stylios,G.K. & Wan,T.R. (1999). The concept of virtual measurement 3D fabric drapeability. *International Journal of Clothing Science and Technology*, 10-18.